Applied Ocean Research **14** (1992) 93–105

A local Fourier approximation method for irregular wave kinematics

Rodney J. Sobey

Department of Civil Engineering, Coastal Engineering Program, University of California at Berkeley, Berkeley, California 94720, USA

(Received 24 October 1990; accepted 7 March 1991)

Significant predictive difficulties have been encountered in the estimation of crest and near-surface kinematics in irregular waves. A review of existing global approximation leads to a recognition of the central role of the free surface boundary conditions in the prediction of the near-surface kinematics. Local approximations that focus on a somewhat smaller segment of the record generally place more emphasis on the free surface boundary conditions and do not compromise local fidelity in the global interest. A local Fourier approximation method for irregular wave kinematics is introduced. The method is rational and not empirical, in that it seeks to exactly satisfy the free surface boundary conditions in a moving local window. Comparisons with predictions from steady wave theory and with laboratory measurements are excellent.

1 INTRODUCTION

The prediction of crest kinematics in irregular waves is a frequent necessity in coastal and ocean hydrodynamics. It is pivotal in the estimation of wave loading on offshore structures and marine pipelines, in the estimation of sediment transport under waves, in analyses of the breaking-wave process and wave-induced circulation in the nearshore zone, and in the interpretation of submerged pressure records.

In many situations, analysis is based on measured or simulated water surface time histories at a fixed location. Spatial measurements of the sea state are most rare and the vast majority of measured field and laboratory records are discrete water surface $\eta(t)$ records from wave staffs or accelerometer buoys at a fixed location. The balance of the wave kinematics (velocities, accelerations and pressures) at the fixed location needs to be estimated from the known $\eta(t)$ trace.

A closely related problem arises in statistical simulation of a random sea state from the linear Gaussian random wave model. Considerable success is achieved in the prediction of the space- and time-varying water surface. Unfortunately, this success does not carry through to the estimation of the near-surface kinematics where a more satisfactory methodology needs to be adopted. Statistical simulation can provide a spatial as well as a temporal description of the sea state. At a fixed location, however, the problem is similar to that defined by a measured record.

The complete problem is the prediction of the wave kinematics at a fixed (x, y, z) location (x, y horizontal, z vertically upwards from the mean water level) beneath a given but irregular water surface profile $\eta(t; x, y)$ at the same horizontal x, y location. Consideration in the present paper is restricted to a subset of this problem where there is no y variation and the direction of both the wave motion and any coexisting Eulerian current coincides locally with the x-axis.

This problem has been addressed by a range of methodoligies. Many are essentially global approximation techniques that focus on a complete measured wave, defined, say, by consecutive zero up-crossings. Others are more local approximations that focus on a somewhat smaller segment of the record.

A brief review of existing global approximations leads to a recognition of the central role of the free surface boundary conditions in the prediction of the near-surface kinematics. Local approximations generally place more emphasis on the free surface boundary conditions and do not compromise local fidelity in the global interest. They have considerable potential in the estimation of irregular wave kinematics.

The present paper introduces a moving, locally steady Fourier approximation method for irregular wave kinematics. The method is compared with existing

Applied Ocean Research 0141-1187/92/$05.00

approaches and shown to have considerable potential in the estimation of wave kinematics, especially in near-surface regions. Comparisons are made with predictions from steady wave theory and with measurements from laboratory experiments.

2 EXISTING METHODOLOGIES FOR IRREGULAR WAVES

Early approaches to the prediction of irregular wave kinematics closely followed the pattern adopted in classical regular progressive wave theory. The discussion is facilitated by recalling the basis of the classical theory.

Background in regular wave theory

The mathematical formulation of regular wave theory is generally cited in an unsteady form, in an (x, z, t) frame that is fixed in space with the z datum at the mean water level (MWL). The water is assumed to be incompressible and irrotational. In primitive form, the dependent variables are the pressure and the velocity components and the field equations are the Euler equations. It is generally more convenient to adopt the velocity potential function $\phi(x, z, t)$ as the dependent variable. The field equation is then the Laplace equation

$$\frac{\partial^2 \phi}{\partial x^2} + \frac{\partial^2 \phi}{\partial z^2} = 0 \tag{1}$$

where the velocity components (u, w) in the fixed frame are $(\partial\phi/\partial x, \partial\phi/\partial z)$.

This field equation is subject to the following boundary conditions:

(i) Bottom boundary condition, representing no flow through the horizontal bed, is

$$w = 0 \quad \text{at } z = -h \tag{2}$$

where $-h$ is the elevation of the bed.

(ii) Kinematic free surface boundary condition (KFSBC), representing no flow through the free surface, is

$$w = \frac{\partial \eta}{\partial t} + u\frac{\partial \eta}{\partial x} \quad \text{at } z = \eta(x, t) \tag{3}$$

where $\eta(x, t)$ is the free surface.

(iii) Dynamic free surface boundary condition (DFSBC), representing constant atmospheric pressure on the free surface, is

$$\frac{\partial \phi}{\partial t} + \tfrac{1}{2}(u^2 + w^2) + g\eta = \bar{B} \quad \text{at } z = \eta(x,t) \tag{4}$$

where g is the gravitational acceleration and $\bar{B}$ is the Bernoulli constant.

(iv) Wave is periodic in space and time, such that

$$\phi(x, z, t) = \phi(x + 2\pi/k, z, t) = \phi(x, z, t + 2\pi/\omega) \tag{5}$$

where k is the wave number and ω is the wave frequency.

(v) Wave maintains a stable profile shape (or permanent form), requiring the wave profile to be symmetric in both x and t about the crest.

Progressive waves of permanent form are steady in a frame of reference moving at the phase speed $C = \omega/k$, with the water surface evolving as

$$\frac{\partial \eta}{\partial t} + C\frac{\partial \eta}{\partial x} = 0 \tag{6}$$

Established regular wave theories (Stokes, Cnoidal, Fourier approximation) generally take advantage of the relative simplicity of the steady formulation where the independent variables are reduced to $x - Ct$ and z. Basis function predictors of the dependent variable (typically the stream function) identically satisfy both the field equation and the bottom boundary condition, together with the permanent form constraint and the periodic lateral boundary conditions. Compatibility conditions designate the wave height and the co-flowing current.

The essential detail of the solution, however, is determined largely by the free surface boundary conditions which must be satisfied along the complete water surface. The complexity of the gravity wave problem is manifested through these free surface boundary conditions, which introduce non-linearity to the problem and are applicable at a free surface that is itself part of the solution. Different orders of the same wave theory are distinguished by the level of approximation to the free surface boundary conditions, higher orders providing enhanced fidelity.

A conflict is immediately identified between the predictive capabilities of regular wave theory and the nature of the solution field. Wave theory consistently predicts that peak magnitude and response extremes in velocities, accelerations and dynamic pressures are located along the free surface. Unfortunately, this region of peak interest in the kinematics and dynamics exactly coincides with the region of maximum uncertainty in the wave theory predictions.

Generalization to irregular waves

The spatial and temporal complexity of irregular waves would initially appear to have little in common with the conspicuous order of regular wave theory. Nonetheless, much of the problem formulation remains appropriate. Irregular waves are by nature unsteady, so that an unsteady formulation is pertinent. The field equation (eqn. (1)), the bottom boundary condition (eqn (2)) and both the free surface boundary conditions (eqns (3) and (4)) continue to be applicable; these constitute the bulk of the mathematical physics. Neither the periodic lateral boundary conditions, nor symmetry about the crest in x and t are appropriate for irregular waves. Further, application of the KFSBC is inconsistent with the present reliance on measured water surface records at a fixed location, as spatial gradients of η are not available from the measured record.

The crucial aspects of the mathematical physics of the regular wave problem are the nonlinear free surface boundary conditions. The close relationship between regular and irregular wave theory guarantees that the free surface boundary conditions will remain a crucial aspect of irregular wave theories.

Global approximations to irregular waves

Methodologies that seek to represent a complete irregular wave, from crest to following crest, from trough to following trough or from zero-crossing to following zero-crossing, are categorized as global.

An obvious candidate is to couple the familiar zero-crossing identification of a wave height and a wave period for an individual wave record with an appropriate steady wave theory prediction for the same height, period, water depth and current. In principle, this is the essence of the design wave approach. As the dominant length and time scales are essentially correct, there is an intuitive expectation that ensuing predictions of crest kinematics have the correct order of magnitude. There can be no expectation, however, that the predictive capability will consistently exceed order-of-magnitude precision. The water surface profile predicted by the force-fitted regular wave theory is unlikely to correspond with the irregular wave profile, so that the free surface boundary conditions will not be satisfied on the actual water surface.

A familiar alternative is the superposition of numerous freely-propagating Airy waves, whose amplitudes, frequencies and phases are determined from a discrete Fourier transform of the irregular wave profile. Temporal periodicity is implicit in the discrete Fourier tranform and the adoption of Airy theory introduces an explicit assumption regarding the nature of the irregular sea state and the ensuing spatial and temporal evolution. Consistent kinematics are available from Airy wave theory. The horizontal velocity, for example, is

$$u(x, z, t) = \sum_n \omega_n \frac{\cosh k_n(h + z)}{\cosh k_n h} \eta_n(x, t) \tag{7}$$

where the η_n water surface components sum to η and each of the n component Airy waves separately satisfy the linear dispersion relationship. Considerable difficulties, however, are encountered at elevations above the MWL, which is the strict upper bound of the Airy solution domain. The hyperbolic function quotients become exceptionally large for the high-frequency (and high wave number) components, leading to substantial high-frequency oscillations in the neighborhood of the crest and the complete failure of Airy wave superposition in the estimation of crest kinematics.[1]

More considered approaches necessitate a return to first principles, as depited by the field equation and boundary conditions. There is no existing global methodology that will accommodate the complete problem and available theories rely on significant relaxations of the complete formulation.

Dean[2] focused on profile asymmetry about the crest, hypothesizing an asymmetric-about-the-crest wave of permanent form with periodic lateral boundary conditions. The permanent form is the key assumption as it infers the spatial x variation from a time history of a dependent variable at a fixed x position. In particular, it implies a unique wave phase speed C, such that variations with x and t in the fixed frame can be combined as $X = x - Ct$ in a steady frame, as in steady wave theory. It also implies a single dominant mode that alone (again as in steady wave theory) satisfies the dispersion relationship, all the higher harmonics being bound wave modes that do not satisfy the dispersion relationship.

Dean introducd a variation on steady Fourier approximation wave theory, assuming that the stream function could be represented as a truncated Fourier series of the form

$$\begin{aligned}\Psi(X, z) = {} & (C_E - C)(h + z) \\ & + \sum_j \sinh jk(h + z)[A_j \cos jkX + B_j \sin jkX]\end{aligned} \tag{8}$$

The profile asymmetry about the crest is introduced through the sine terms in the Fourier series, which do not appear in the related Fourier approximations steady wave theory. The field equation and bottom boundary condition remain satisfied exactly and the Fourier coefficients are determined numerically to best fit the kinematic and dynamic free surface boundary conditions at the known water surface nodes. Dean applied this methodology to a complete measured wave from trough to following trough.

Lambrakos[3] introduced a variation on the Dean approach, assuming that the global spatial as well as temporal evolution can be represented in the fixed frame by the velocity potential function

$$\begin{aligned}\phi(x, z, t) = {} & \sum_{j,l} \cosh jk(h + z)[A_{jl} \cos (jkx - l\omega t) \\ & + B_{jl} \sin (jkx - l\omega t)]\end{aligned} \tag{9}$$

which introduces a combination of freely propagating (subscript l) and bound (subscript j) wave modes, but excludes current. The specific assumption regarding the nature of the spatial evolution is necessary to utilize the unsteady form of the KFSBC (eqn 3), which includes the spatial gradient of the water surface. In addition, the nominally separate free modes are in fact prescribed by Lambrakos in the manner of Fourier analysis, the fundamental frequency being $\omega = 2\pi/T$, where T is the duration of the measured record. While this approach may be numerically successful, any expectation of physical success has been substantially compromised by the pre-determination of the spatial evolution and the mix of free and bound modes.

The complete numerical field solution of Forristall[1] similarly requires a specific assumption regarding the nature of the spatial evolution. Several strategies for the estimation of the $\eta(x, t)$ surface were considered, including the linear Gaussian random wave model and a second-order correction (in the deep-water Stokes sense) to this linear surface, following Sharma and Dean.[4] Given a complete description of the $\eta(x, t)$ surface and an assumption of periodic lateral boundary conditions at adjacent troughs, the solution domain is completely defined. Forristall noted that the problem formulation was closed without imposition of the DFSBC, as a direct consequence of the specification of the $\eta(x, t)$ surface.

A full field solution of the Laplace equation under such conditions is numerically straightforward but time-consuming. The boundary integral method would perhaps be more efficient, especially as interest is focused on the rather limited region of the solution domain near the crest. Forristall[5] has extended this methodology to two horizontal spatial dimensions with the $\eta(x, y, t)$ surface estimated from a directional spectral description provided by the Gaussian random wave model (superposition of free modes) with second-order (bound wave modes) corrections. This procedure becomes computationally intensive (Cray + vector processing).

Local approximations to irregular waves

Methodologies that seek only to represent the local behavior of an irregular wave are categorized as local. Given that significant problems such as crest kinematics are strongly related to local errors in the free surface boundary conditions, there is intrinsic value in pursuing such an approach. Such methodologies compromise applicability in a global sense in an effort to achieve fidelity in a local sense. Note that this contrasts with the general approach of steady wave theory where local fidelity (especially near the wave crest) is perhaps sacrificed in the global interest.

One form of local approximation, the so-called 'stretching' method of Wheeler,[6] has found considerable favor as a pragmatic approach to the prediction of irregular wave kinematics. Recognizing that the failure of Airy superposition was contributed by extrapolation of the hyperbolic function quotients beyond the upper bound of the Airy solution domain, Wheeler introduced an empirical transformation on the local elevation such that it never exceeds the MWL. The horizontal velocity is predicted as

$$u(x, z, t) \;=\; \sum_j \omega_n \frac{\cosh \alpha k_n h}{\sinh k_n h}\, \eta_n(x, t) \qquad (10a)$$

where $\alpha = (h + z)/(h + \eta)$, the transformation depending upon the local water surface elevation. As a result of this transformation, the field equation is no longer satisfied by the predictive equations for the kinematics. The relocation of the local water surface at the MWL, however, sharply reduces errors in the free surface boundary conditions, as Airy theory imposes the free surface boundary conditions at the MWL. Wheeler does not give estimators for the balance of the kinematics, but consistent estimators for the vertical velocity and the horizontal acceleration would be

$$w(x, z, t) \;=\; \sum_j \omega_n \frac{\sinh \alpha k_n h}{\sinh k_n h}\, \hat{\eta}_n(x, t) \qquad (10b)$$

and

$$\frac{\partial u}{\partial t}(x, z, t) \;=\; \sum_j \omega_n^2 \frac{\cosh \alpha k_n h}{\sinh k_n h}\, \hat{\eta}_n(x, t) \qquad (10c)$$

respectively, in which the $\hat{\eta}_n$ sum to $\hat{\eta}$, is the Hilbert transform of η. Variations on 'Wheeler stretching' have been introduced by Chakrabarti,[7] Gudmestad and Connor,[8] Lo and Dean[9] and Rodenbusch and Forristal (1986).[10]

Airy wave theory has also been used with locally defined, rather than globally defined, parameters. Airy theory predicts that the water surface profile is

$$\eta(x, t) \;=\; a \cos(kx - \omega t + \theta) \qquad (11)$$

where θ is the phase. At a fixed location, the local parameters are the amplitude a, the frequency ω and the net phase $kx + \theta$. Daemrich *et al.*[11] contracted the familiar zero-up-crossing identification of a complete wave to a zero-up-and-down-crossing identification of consecutive half waves. Different amplitudes, frequencies and phases were assigned to each half wave, crest half waves typically having a larger amplitude and higher frequency. Nielsen[12,13] further localized the definition of amplitude, frequency and phase to a moving window of three consecutive water surface observations, which is sufficient to uniquely define the local amplitude, frequency and phase. Even with local definitions of amplitude, frequency and phase, Airy wave theory is not especially successful in the prediction of crest kinematics. The problem is intrinsic to the theory, which is a first-order approximation where residual errors in the free surface boundary conditions are not small for finite amplitude waves. Nielsen couples local Airy parameters with vertical coordinate stretching

Fenton[14] has presented a local approximation methodology that is theoretically attractive. The wave field is assumed to be locally steady with local phase speed C, such that variations with x and t in the fixed frame can be combined as $X = x - Ct$ in a locally steady frame, as in steady wave theory. The local solution is presented by a truncated polynomial series for the complex potential function

$$\Phi(X, z) + i\Psi(X, z) \;=\; \sum_j \frac{a_j}{j+1}\,[X + i(h + z)]^{j+1} \qquad (12)$$

where the a_j polynomial coefficients are real. These basis functions satisfy the field equation and bottom boundary condition exactly. The polynomial coefficients are determined numerically to best fit the kinematic and dynamic free surface boundary conditions at the known water surface nodes. Fenton actually considered the more complicated problem of estimating the water surface as well as the balance of the kinematics from a measured pressure time history at a submerged location. This is a familiar problem associated with bottom pressure wave recorders, for which Airy wave theory has been consistently used — even in shallow water. This polynomial procedure was shown to cope reasonably well for longer waves, where a polynomial variation in the vertical is also a feature of Cnoidal wave theory. It does not do so well for shorter waves, where the vertical variation tends to exponential and where presumably the hyperbolic sine variation of Stokes theory is more suitable. The reverse problem, that of estimating submerged kinematics from a measured water surface time history, is an arguably simpler problem, having the nature of interpolation rather than extrapolation.

3 A LOCAL FOURIER APPROXIMATION METHOD

Several constraints are inherent in any methodology that seeks to predict wave kinematics from a measured water surface time history at a fixed location. A major concern must be fidelity in the mathematical physics of surface gravity waves. This is assured by a predictive scheme that satisfies the field equation throughout the fluid domain, the bottom boundary condition at the bed and the free surface boundary conditions at the water surface. Fidelity in representation of the KFSBC and the DFSBC at the given location of the water surface is especially crucial. Significant errors are introduced by imposing the free surface boundary conditions at the MWL or along a regular wave profile to which the irregular wave trace is associated.

It is also necessary to introduce a specific assumption regarding the nature of the associated spatial evolution. Such an assumption is required because of the spatial gradient term in the KFSBC. This assumption, however, should not be allowed to dominate the solution methodology. The present methodology is a pragmatic and rational response to these constraints. Firstly, it is a local approximation method. This enhances fidelity in representation of the crucial free surface boundary conditions and minimizes the influence of the necessary spatial evolution assumption. Secondly, it is a generalization of the widely successful (but global) Fourier approximation method for regular waves, which has almost universal applicability for both deep and shallow water waves and for co-flowing uniform currents. The methodology is extended to complete irregular water surface profiles by means of a moving window of duration τ, which is small in comparison with the local zero-crossing period.

Local problem formulation

The basis of the present method is the representation of the velocity potential function within each window as

$$\phi(x, z, t) = C_E x + \sum_{j=1}^{J} A_j \frac{\cosh jk(h+z)}{\cosh jkh} \times \sin j(kx - \omega t) \tag{13}$$

This representation is familiar from global Fourier wave theory (e.g. Sobey[15]), where C_E is the spatially uniform Eulerian current, h is the water depth, A_j are the Fourier coefficients (of which there are J), k is the wave number, ω is the wave frequency and (x, z) is the spatial position in the fixed frame. The current and the water depth define the local propagation medium and must be specified. In Fourier wave theory, ω, k and the A_j, together with the Bernoulli constant $\bar{B}$, constitute a defining set of parameters that have unique values. In the local Fourier approximation method, the defining set of parameters is no longer constant but may vary from window to window.

Within each window, the eqn (13) basis functions exactly satisfy both the field equation throughout the fluid domain and the bottom boundary condition, regardless of the numerical values of the defining set of parameters. The defining set of parameters are determined within each window to best satisfy the free surface boundary conditions at the measured elevations of the free surface within the window.

For each window solution, the given information is the local water depth h and the local co-flowing uniform Eulerian current C_E, together with a set of water surface elevations η_i, where the $i = 1, 2, \ldots I$ are distributed over the local window of duration τ.

The specific equations defining the window solution are the kinematic free surface boundary condition at each free surface node

$$f_i^{K}(\omega, k, kx, A_j) = w_i - \frac{\partial \eta_i}{\partial t} - u_i \frac{\partial \eta_i}{\partial x} = 0 \tag{14}$$

and the dynamic free surface boundary condition at each free surface node

$$f_i^{D}(\omega, k, kx, A_j) = \frac{\partial \phi_i}{\partial t} + \tfrac{1}{2}u_i^2 + \tfrac{1}{2}w_i^2 + g\eta_i - \bar{B} = 0 \tag{15}$$

in which

$$\frac{\partial \phi_i}{\partial t} = -\sum_j (jw)^2 A_j \frac{\cosh jk(h+\eta_i)}{\cosh jkh} \cos j(kx - \omega t_i)$$

and the velocity components are, respectively,

$$u_i = u(x, \eta_i) = C_E + \sum_j jkA_j \frac{\cosh jk(h+\eta_i)}{\cosh jkh} \times \cos j(kx - \omega t_i)$$

and

$$w_i = w(x, \eta_i) = \sum_j jkA_j \frac{\sinh jk(h+\eta_i)}{\cosh jkh} \times \sin j(kx - \omega t_i)$$

The Bernoulli constant in the DFSBC is not a free parameter, being related to the other solution parameters through the exact integral relationship[16]

$$\bar{B} = g\bar{\eta} + \tfrac{1}{2}\langle u_b^2 \rangle \tag{16}$$

where $\bar{\eta}$ is the MWL and $\langle u_b^2 \rangle$ is the mean-square horizontal bed velocity. The MWL is zero from the present choice of vertical datum and, using eqn (13) at $z = -h$, the local Bernoulli constant becomes

$$\bar{B} = \tfrac{1}{2}C_E^2 + \tfrac{1}{4}\sum_j \left(\frac{jkA_j}{\cosh jkh}\right)^2 \tag{17}$$

The temporal and spatial gradients of the water surface in the KFSBC equations remain to be specified. Temporal gradients can reasonably be estimated from the water surface time history. Cubic spline interpolation among the measured water surface nodes conveniently provides consistent and smoothly varying estimates of both η and $\partial\eta/\partial t$, and has been routinely adopted.

Spatial gradients are not available from the measured record at a single site and some assumption is necessary. A lowest order candidate would be to drop the nonlinear $u\partial\eta/\partial x$ term from the KFSBC, as in linear weave theory. An attractive alternative is a locally steady assumption that imposes eqn (6) in each local window and relates the spatial and temporal gradients as

$$\frac{\partial\eta}{\partial x} = \frac{1}{C}\frac{\partial\eta}{\partial t} \tag{18}$$

where $C = \omega/k$ in the local window. The steady profile assumption is not imposed beyond the local window and will not dominate the solution methodology, as it does, for example, in the Dean[2] and Lambrakos[3] methodologies.

Aspects of the numerical solution

This equation set is nonlinear and implicit. The primitive unknowns in the local window are ω, k, x and the A_j, of which there are J. The spatial phase always occurs in the combination kx and experience indicated some slight numerical convenience in choosing the set of $3 + J$ unknowns as ω, k, kx and the A_j. There are two independent equations potentially available at each of the η observations within the local window, of which M are selected for the numerical solution. The problem is uniquely defined for $M = 3 + J$ and overspecified for $M > 3 + J$. In recognition of the certain existence of error bands about the measured water surface elevations, some overspecification may be advantageous.

The numerical problem posed by the solution of such a set of simultaneous implicit nonlinear algebraic equations is categorized as nonlinear optimization. Suitable algorithms are available in a number of the standard subroutine libraries. Algorithms HYBRJ and LMDER from the MINPACK subroutine library are suitable choices for the present study. These algorithms are mature, routinely successful and commonly available. The subroutine HYBRJ finds the zeros of a set of N nonlinear algebraic equations in N unknowns by a modification of the Powell hybrid method. The subroutine LMDER finds a least-squares solution of M nonlinear algebraic equations in N unknowns ($M \geqslant N$) by a modification of the Levenberg-Marquardt algorithm. Both algorithms were utilized in double precision and both required calculation of the Jacobian as well as the functions. The least-squares algorithm is in principle suitable for both uniquely defined and overspecified problems.

Using only the measured water surface elevation, the choice of M largely dictates the width of the local window. Unfortunately, this compromises any systematic efforts in error control and may also degrade the local approximation character of the methodology. A more satisfactory approach is to restrain the width of the local window and achieve the desired local resolution by interpolation within this window. Cubic spline interpolation has been routinely adopted. It provides consistent estimates of both η_i and $\partial\eta_i/\partial t$ together with a measure of flexibility in error control. The width for each local window is constrained at the lower end by the need to resolve the local curvature of the water surface.

From a strictly numerical viewpoint, the only constraint on the choice of order J and the local window width τ is the $M \geqslant 3 + J$ requirement. There is a clear expectation, however, that an appropriate choice of these parameters will be dependent upon the physical nature of the water surface time history together with the local resolution of the measured record. It is accordingly convenient to identify a particular local Fourier (**LF**) solution as **LF**(J; τ, M). With the cubic spline interpolation of the water surface record, the time location of individual windows is independent of the order and the window width. It remains necessary however to provide adequate resolution to capture the temporal variation in the near-surface kinematics. Note that adjacent windows will overlap where the window width exceeds the output resolution.

Given that a solution exists, these are two (and largely endemic) difficulties with any optimization algorithm.

The nature of these difficulties is well known but guaranteed recipes for their resolution are not. Measures that are specific to the particular problem are often required. Such is certainly the case in the present problem.

The first difficulty is the difference in physical dimensions and relative magnitudes of the dependent variables. This has been minimized by redefining the variables and the implicit algebraic equations in dimensionless form, in terms of the local zero-crossing period T_z and the gravitational acceleration. This does not influence the relation among the A_j Fourier components, which are expected to remain a monotonically decreasing sequence.

A second difficulty is potential convergence to physically spurious solutions, a difficulty that increases with the order of the problem. Spurious solutions might be identified by negative values for either the frequency or the wave number, by spatial phases that sharply diverge from the general trend, or by higher order Fourier coefficients that are either large or negative. Spurious solutions can often be avoided in unconstrained optimization by careful selection of the initial estimate and by enhanced numerical precision in computation of both the functions and the Jacobian. Enhanced numerical precision was a routine practice, with all computations in double precision and the Jacobian determined analytically and not by difference approximation.

Several strategies for the selection of initial solution estimates were investigated. Global Airy theory based on zero-crossing estimates of wave height H and period T_z is routinely successful only for wave profiles that are quite close to deep-water Stokes profiles. Spurious solutions are common for profiles with visually minor irregularities or for profiles with identifiable crest steepening and trough flattening. A global curve-fit to a higher order Stokes profile is only marginally more successful. The converged solution for the neighboring window or a Taylor series extrapolation of this solution might be expected to provide a reasonable initial estimate. Unfortunately, this approach has rather erratic success, having particular difficulty in regions of sharp profile curvature. Further, once a spurious solution is achieved, this strategy provides a strong bias towards spurious solutions in subsequent windows.

Difficulties were most consistently avoided by a strategy that largely ignored the neighboring window solution and established initial solution estimates from the local profile elevation η and gradient $\partial\eta/\partial t$, together with the Airy approximations to the free surface boundary conditions, namely

$$\begin{aligned} w - \frac{\partial \eta}{\partial t} &= 0 \qquad \text{at } z = 0 \\ \frac{\partial \phi}{\partial t} + g\eta &= 0 \qquad \text{at } z = 0 \end{aligned} \tag{19}$$

for the KFSBC and DFSBC, respectively. Using eqn (13) with $J = 1$ and solving for A_1 and kx in terms of ω and k gives

$$\begin{aligned} A_1 &= \sqrt{\left(\frac{\partial\eta/\partial t}{k \tanh kh}\right)^2 + \left(\frac{g\eta}{\omega}\right)^2}, \\ kx &= \tan^{-1}\left(\frac{(\partial\eta/\partial t)/(k \tanh kh)}{g\eta/\omega}\right) \end{aligned} \tag{20}$$

The estimate of kx was adjusted by 2π as appropriate to maintain consistency with the neighboring window. The initial estimate of the wave frequency was set at $2\pi/T_z$, with k estimated from ω by the Airy dispersion relationship. Initial estimates of the higher order Fourier coefficients were $A_j = A_1/10^{j-1}$, respectively. The success of this strategy was sometimes tenuous and cannot be categorized as routine. Indeed, this was the anticipated nature of the separate nonlinear optimization problems in each local window, especially given the inevitable error bounds on estimates of η and $\partial\eta/\partial t$.

Where the strategy failed, it was generally clear in the first few iterations that the algorithm was heading for a spurious solution. These trends were arrested by the definition of physically appropriate inequality constraints on the solution parameters and the imposition of a penalty on the functions when these constraints were violated.

Difficulties are almost invariably associated with markedly irregular profile segments. These were accommodated by the introduction of local smoothing in various guises, the measures adopted being closely analogous to the routine procedures in establishing smooth spectral estimates from a sequence of measured η observations. Both the raw water surface record and the window solutions were subjected to a moving average filter whose width was related to the width of the local windows. The half width of the filter was chosen as $L \times \text{Nint}[(\tau/\Delta t - 1)/2]$, where the function Nint identifies the nearest non-zero integer. Δt is the time step of the data sequence, which is determined by the available η record on input but may be freely selected on output. A suitable choice for the filter weight L would recognize the precision of the available η record; it was set typically to 1 for laboratory and field records, but could be set to 0 to suppress filtering.

Some further smoothing was also implicit in the choice of J and M. Numerical experience rapidly showed there was no discernable advantage in adopting J values in excess of 3. With 3 as an upper bound on J, the distribution of points within each local window that is shown in Fig. 1 was adopted as a standard. The superscripts in this figure also indicate the sequence in which the KFSBC (marked as K^i) and the DFSBC (marked as D^i) equations were utilized. For example, at $M = 5$, KFSBC equations were utilized at local time $t = -0{\cdot}5\,\tau$, $0{\cdot}0$ and $0{\cdot}5\,\tau$ and DFSBC equations at $t = -0{\cdot}5\,\tau$ and $0{\cdot}5\,\tau$. Local time was set to zero in the middle of each window with the spatial phase kx defined accordingly. The exact HYBRJ and least-squares LMDER algorithms were

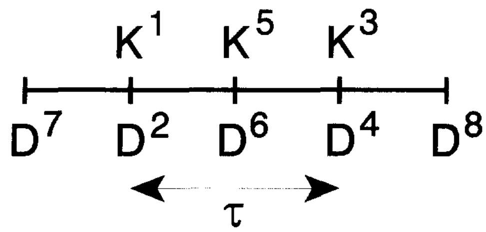

Fig. 1. Distribution of points and free surface boundary conditions within local window.

used sequentially, starting with HYBRJ with $M = 3 + J$ and followed by LMDER with $M = 6$, then 7 and 8 until convergence was achieved. The M = 7 and 8 options are contingency provisions that extend the width of the local window to $t = \pm\tau$, introduced specifically to accomodate profile segments with limited curvature in the trough and zero-crossing regions. The extended points use only the DFSBC and avoid using the KFSBC, which would unnecessarily extend the spatial extent of the locally steady assumption. With a local window of adequate width (typically 0·1 T_z), these wider window options are rarely utilized.

4 EVALUATION OF METHOD

Theoretical kinematics

Near-exact solutions for regular progressive waves provide an opportunity to evaluate the potential of the local approximation technique without the complicating influence of error bands on measured water surface profiles.

Two relatively extreme waves have been selected for comparison, respectively in deep and shallow water. Details are listed in Table 1. The kinematics were predicted by Fourier approximation wave theory.[15]

The input data to the local approximation code was the theoretical water surface profile at a discrete time step of 0·5 s, corresponding to typical field measurement programs. The record segment was centered on a crest and extended from the previous crest to the following crest. The water depth and uniform current were also specified. The width of the local window was set at 0·1 T_z (i.e. 1 s here) and solutions were established for local windows extending from the profile zero-down-crossing immediately preceding the central crest to the profile zero-up-crossing immediately following the central crest. It is appropriate in these computations to suppress smoothing (setting $L = 0$) as the water surface elevations are known quite precisely.

The kinematics are most extreme at the water surface and any theory is expected to be least satisfactory at this location. Attention is accordingly focused on comparisons between predicted and theoretical kinematics along the water surface.

Figure 2 shows a comparison of the local Fourier approximation predictions with the theoretical kinematics for the deep-water regular wave. These are **LF**(2) solutions, the truncation order J for these local solutions being 2. The solid lines are the theoretical predictions and the markers identify the local approximation method. Part (a) shows the water surface profile and the discrete input record for the local approximation code. Parts (b) and (c) show the horizontal and vertical components of the velocity along the water surface. Part (d) shows the horizontal acceleration along the water surface. Agreement throughout is excellent, the only minor blemish being the horizontal velocity at the trough.

Another perspective on the utility of the local approximation method is provided by a comparison with the Wheeler stretching predictions (eqn (10)) under comparable conditions. These predictions are shown in Fig. 3(b) through (d). They were based on exactly the same input record segment (Fig. 3(a)) and smoothing (none) as the Fig. 2 predictions. Errors are systematic and reach magnitudes of order 20% on the high side for velocities and rather more for accelerations. Given the empirical nature of the stretching methodology, a better result cannot be expected for reasonably extreme waves.

The shallow water wave provides an even more demanding test of the local Fourier methodology. The near-crest kinematics are relatively extreme and vary rapidly with time in comparison to the near-trough kinematics. This wave is quite close to the limit wave for this water depth and current. The **LF**(3) predictions in Fig. 4, however, are again excellent, especially for the crest kinematics. Minor problems in the horizontal velocity prediction at the trough and on the trough side of profile zero-crossings remain apparent. These errors are small and isolated to a few locations, but are nonetheless symptomatic of the often tenuous nature of convergence for the separate and unrelated nonlinear optimization problems in each local window.

A remarkable feature of the local Fourier approximation methodology is the low truncation order necessary to achieve excellent precision for quite extreme waves. Local Fourier truncation orders of 2 in deep water

Table 1. Characteristics of Theoretical Regular Waves

Wave	*Wave height (m)*	*Water depth (m)*	*Wave period (s)*	*Uniform current (m/s)*	*Truncation order*
Deep	20	100	10	0	10
Shallow	3	5	10	−2	18

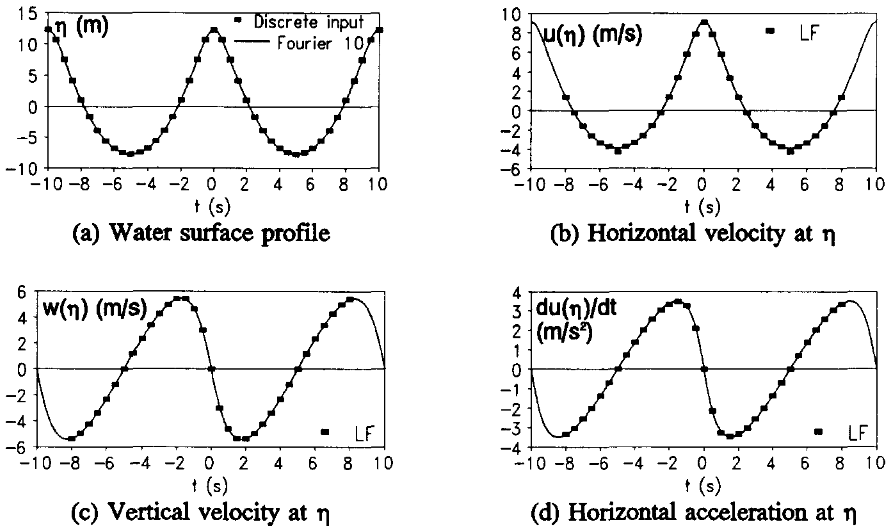

Fig. 2. Theoretical kinematics and **LF** predictions for the deep-water regular wave.

and 3 in shallow water were sufficient to achieved comparable accuracy to global Fourier truncation orders of 10 and 18, respectively (see Table 1). This is achieved of course through local values for the frequency, the wave number, the spatial phase and the Fourier coefficients. This local nature of the solution is well illustrated in Fig. 5 which shows the evolution of the window solution for the shallow water wave.

Measured kinematics

Further illustrations of the utility of the **LF** methodology is provided by comparisons with laboratory measurements of near-surface kinematics in irregular waves. It is necessary in these comparisons that the x locations of the measured water surface trace and the near-surface kinematics correspond. Evaluation of the results would otherwise be distorted by the need to adopt some assumption regarding the nature of the spatial evoluton.

Tørum and Skjelbreia[17] obtained LDV measurements of near-surface kinematics in a laboratory wave flume. In the record segment available for analysis, the water depth was 1·3 m and the waves were a random simulation of a mean Jonswap spectrum with a peak period of 1·8 s and significant wave height of 0·2 m. Simultaneous measurements were made at the same x location of the water surface trace $\eta(t;\ x)$ and the $u(t;\ x,\ z)$ and $w(t;\ x,\ z)$ velocity components at an elevation of $z = -0{\cdot}15$ m. The sampling interval was 0·025 s. The mass flux constraint imposed by the flume generates a small return current in the flume to compensate for the forward mass flux in the trough–crest region. The co-flowing Eulerian current was estimated as $C_E = -0{\cdot}056$ m/s from the time average of the horizontal velocity trace. The input water surface trace is shown in Fig. 6(a). The markers in Fig. 6(b) through 6(d) show the **LF**(3) predictions for horizontal velocity, vertical velocity and horizontal acceleration, respectively, at $z = -0{\cdot}15$ m. The filter

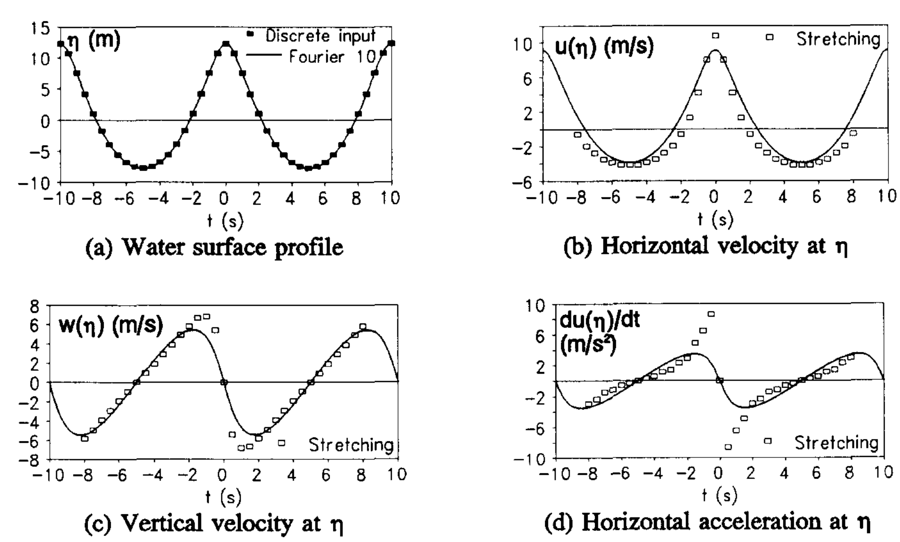

Fig. 3. Theoretical kinematics and Wheeler stretching predictions for the deep-water regular wave.

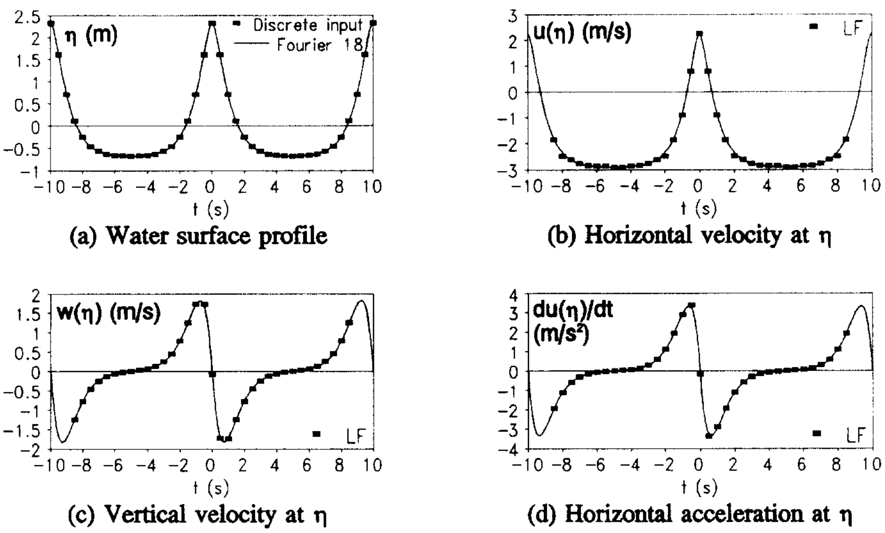

Fig. 4. Theoretical kinematics and **LF** predictions for the shallow-water regular wave.

parameter L was 1. The continuous lines are the LDV measurements. The agreement is generally good, though certainly not perfect. Acceleration was not measured.

The second data set is unpublished data in 1984 from the Delft Hydraulics Delta Flume, the very large outdoor wave facility at the De Voorst laboratory. In the record segment available for analysis, the water depth was 5·0 m and the waves were a random simulation of a mean Jonswap spectrum with a peak period of 6·0 s and significant wave height of 0·8 m. Simultaneous measurements were made at the same x location of the water surface trace $\eta(t;\, x)$ and the $u(t;\, x,\, z)$ and $w(t;\, x,\, z)$ velocity components at an elevations of $z = -1{\cdot}75$ m and $z = -3{\cdot}50$ m. The sampling interval was 0·04 s. The water surface trace was measured by a profile-following wave gage and the kinematics by Colnbrook velocity meters laterally offset by 1.75 m from the wave gage. The co-flowing Eulerian current was estimated as $C_E = -0.009$ m/s from the time average of the horizontal velocity traces. The input water surface trace in Fig. 7(a) shows a trough-to-crest height in excess of 1 m, significant profile asymmetry, notable oscillation at the leading trough and a somewhat deeper trailing trough. The markers in Fig. 7(b) through 7(d) show the **LF**(3) predictions for horizontal velocity, vertical velocity and horizontal acceleration, respectively, at $z = -1{\cdot}75$ m and $z = -3{\cdot}50$ m. The filter parameter L was again 1. The continuous lines are the velocity meter measurements. Once again, the agreement is generally good, especially for the vertical velocity traces. Agreement is less satisfactory for horizontal velocity at the wave crest.

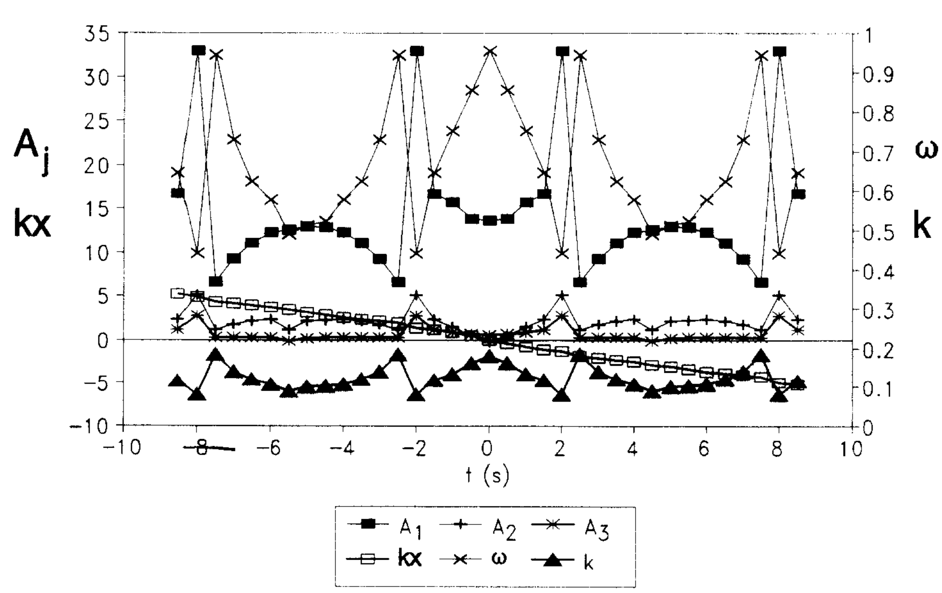

Fig. 5. Evolution of window solution for the shallow-water regular wave.

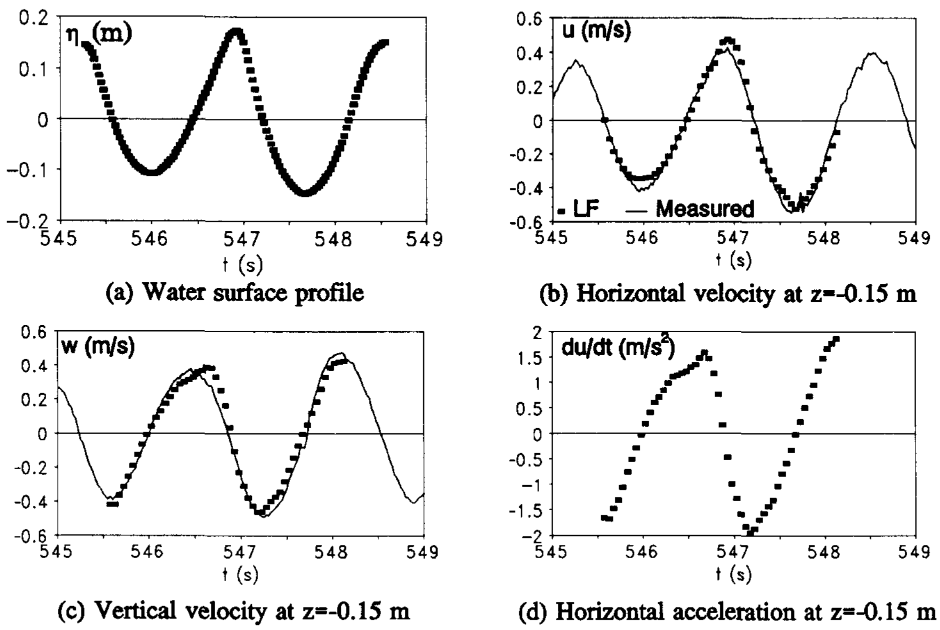

Fig. 6. Measured kinematics and **LF** predictions for a laboratory wave of Tørum and Skjelbreia.[17]

Potential error sources

Potential sources or error in the **LF** methodology are readily apparent. Some minor numerical uncertainty was identified in comparisons with theoretical waves in Fig. 2 and 4. This uncertainly must be expected to be rather more widespread with irregular profiles. Further, there are error bands on both the measured water surface trace, on which the **LF** predictions are based, and on the measured kinematics. The light filtering cannot compensate for all of this.

In addition to these largely numerical errors, potential physical errors much be acknowledged. It is explicitly assumed in the formulation that the higher order Fourier modes are locally bound and not free modes. Coexisting free modes are ignored but may contribute significantly, especially in the crest and trough regions if they are propagating in opposition to the dominant waves. In imposing the kinematic free surface boundary condition, it was necessry to assume that the profile in each window was locally steady. While this is certainly an error source, it influences only the advective term in the KFSBC, whose contribution would only rarely be dominant.

As the horizontal velocity prediction seems most vulnerable to error, the possibility of an unsteady propagation medium must also be recognized. Longer period modes in the flume may not be distinguishable in the water surface trace and would not be resolved in the local windows. They may significantly contribute, nonetheless, to the horizontal velocity structure.

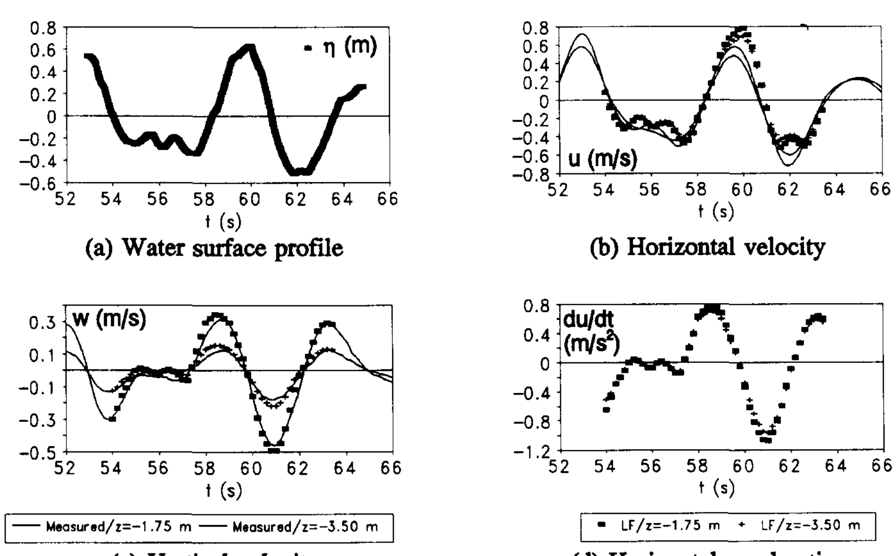

Fig. 7. Measured kinematics and **LF** predictions for a laboratory wave in Delft Hydraulics Delta Flume (1984).

No attempt is presently made to accommodate the directional structure of real sea states and current fields. A real sea state involves a spread of wave directions about an identifiable dominant direction. More complicated sea states may be directionally bi-modal. In addition, the co-existing current may not coincide with either of the dominant wave directions. The present method is predicated on the availability of a measured water surface record, which includes no directional information, and ignores the existence of any directional structure in the wave and current field. It is assumed that the directions of the current and secondary wave field correspond with or directly oppose the primary wave direction.

No attempt is presently made to accommodate the directional structure of real sea states and current fields. A real sea state involves a spread of wave directions about an identifiable dominant direction. More complicated sea states may be directionally bi-modal. In addition, the co-existing current may not coincide with either of the dominant wave directions. The present method is predicated on the availability of a measured water surface record, which includes no directional information, and ignores the existence of any directional structure in the wave and current field. It is assumed that the directions of the current and secondary wave field correspond with or directly oppose the primary wave direction.

Whether the **LF** methodology can be extended to directionally complex sea state remains an open question. In principle, such an approach may be feasible if the current and dominant wave directions are known. Interaction terms would, however, increase the number of unknowns and complicate the already tenuous numerical solutions.

5 APPLICATIONS

The particular value of the **LF** methodology is the provision of predicted surface and subsurface kinematics where only the water surface time history is known. Two classes of problem may be identified. In the first, the water surface trace may be available from a field or laboratory measurement program. The measurement of water surface elevations in the field and the laboratory is now a relatively routine practice. The direct measurement of kinematics is more difficult. Neither is it cost effective, as there is both z and t variation at a particular site as well as horizontal and vertical velocities, horizontal and vertical accelerations and dynamic pressure to be measured.

In the second class of problem, a water surface trace may be available from a simulation of the water surface, for example from the Gaussian Random Wave Model. The GRWM provides realistic simulations of water surface time histories and of subsurface kinematics at elevations somewhat below the wave trough level. As discussed previously, however, the predictive capability of the GRWM for crest kinematics is destroyed by high frequency oscillations. The **LF** methodology will provide appropriate predictions of crest-to-trough kinematics in this situation.

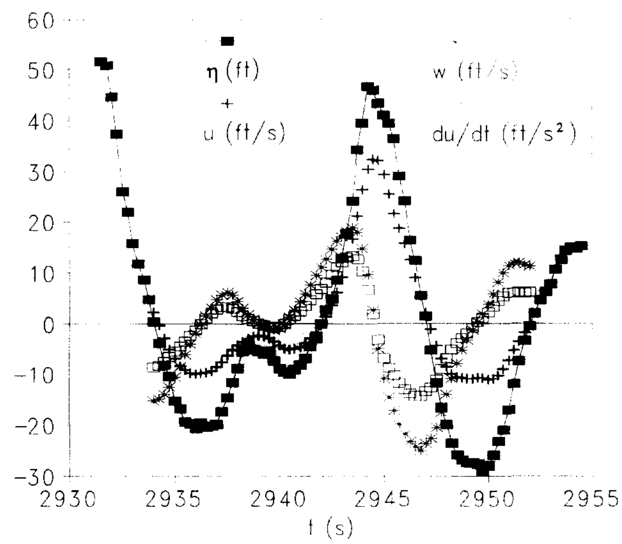

Fig. 8. LF predictions for a measured wave during Hurricane Camille (1969).

Among the largest waves that have been measured were recorded during Hurricane Camille in the Gulf of Mexico on 16 August 1969. Two waves towards the end of the record are especially extreme, one (with the higher crest) having a zero-crossing wave height of 22·0 m and the following wave (with a lower crest but a deeper trough) a zero-crossing wave height of 23·0 m. These waves have become very well known among ocean engineers and are perhaps the highest waves that have yet been measured.

The second and higher of these two waves provides a worthwhile applications example. The measured water surface record is shown as the continuous line with markers in Fig. 8. The sampling interval was 0·25 s and the water depth was 340 ft. No current was measured and zero current was assumed. The markers in Fig. 8 show the **LF**(3) predictions for horizontal velocity, vertical velocity and horizontal acceleration at the water surface, where these variables will be most extreme. The filter parameter L was 1. The **LF** prediction are visually plausible but there are neither measurements nor theory for confirmation.

6 CONCLUSIONS

The need for a predictive capability in irregular wave kinematics is most imperative at the water surface where velocities, accelerations and dynamic pressures all reach their peak values. Unfortunately, predictive methodologies are most vulnerable at the water surface, as a direct consequence of approximations in the imposition of the nonlinear free surface boundary conditions. Any methodology for the prediction of irregular wave kinematics that is both rational and viable must give appropriate attention to the free surface boundary conditions.

Global and local methodologies are distinguished. Local methods do not compromise local fidelity in the representation of the free surface boundary conditions in the global interest. Global methods, which closely follow regular wave theory, are less attractive for irregular wave kinematices.

A local Fourier approximation (**LF**) methodology is presented for the prediction of irregular wave kinematics beneath a given water surface trace in a unidirectional wave field. Separate solutions are established in narrow and sequential local windows along the water surface. The local solution parameters are established numerically from the kinematic and dynamic free surface boundary conditions imposed at the measured water surface elevations within each window. The dynamic free surface boundary condition is imposed exactly. The kinematic free surface boundary condition includes a spatial gradient of the water surface elevation which is not available from a measured water surface trace at a fixed location. This spatial gradient is accommodated by assuming that the profile is locally steady within each narrow window, but not globally steady across the complete wave. The method is strictly rational in its reliance on the field equation and the bottom and free surface boundary conditions. There are no empirical elements.

Comparisons with prediction from steady regular wave theory are excellent and comparisons with measured laboratory kinematics established the utility of the **LF** methodology.

The approach is applicable to both measured and simulated water surface traces. An adaption of the method would also be appropriate to the estimation of the water surface trace and the balance of the kinematics from a measured subsurface pressure record.

ACKNOWLEDGEMENTS

Measured wave and wave kinematics data were provided to this study from several sources. The data Figs 6, 7 and 8 were provided by Ove Gudmestad (Statoil, Stavanger, Norway), Gert Klopman (Delft Hydraulics, Emmeloord, The Netherlands) and Chuck Petrauskas (Chevron, La Habra, California), respectively. Additional field data provided by Michel Olagnon (IFREMER, Brest, France) and Chuck Petrauskas were not used in the paper but served to establish the limitations of the present approach in accomodating bi-modal sea states in ambient currents. The encouragement and support of these people is sincerely appreciated.

REFERENCES

1. Forristall, G.Z., Irregular wave kinematics from a kinematic boundary condition fit (KBCF). *Appl. Ocean Res.*7 (1985) 202–12.
2. Dean, R.G., Stream function representation of nonlinear ocean waves. *J. Geophys. Res.*, **70** (1965) 4561–72.
3. Lambrakos, K.F., Extended velocity potential wave kinematics. *J. Waterway, Port, Coastal and Ocean Div., ACSE*, **107** (1981) 159–74.
4. Sharma, J.N. & Dean, R.G., Development and evaluation of a procedure for simulating a random directional second order sea surface and associated wave forces. Ocean Engineering Report 20, University of Delaware.
5. Forristall, G.Z. Kinematics in the crests of storm waves. *Proc. 20th Int. Conf. on Coastal Engineering, Taipei, ASCE*, **1** (1986) 208–222.
6. Wheeler, J.D., Method for calculating forces produced by irregular waves. *Proc. 1st Annual Offshore Technology Conference, Houston*, **1** (1969) 71–82.
7. Chakrabarti, S.K., Discussion on 'Dynamics of single point mooring in deep water'. *J. Waterways, Harbors and Coastal Eng. Div., ASCE*, **97** (1971) 588–90.
8. Gudmestad, O.T. & Connor, J.J., Engineering approximations to nonlinear deepwater waves. *Appl. Ocean Res.*, **8** (1986) 76–88.
9. Lo, J. & Dean, R.G., Evaluation of a modified stretched linear wave theory. *Proc. 20th Int. Conf. on Coastal Engineering, ASCE*, **1** (1986) 522–36.
10. Rodenbusch, G. & Forristall, G.Z., An empirical model for random directional wave kinematics near the free surface. *Proc., 18th Annual Offshore Technology Conference, Houston*, **1** (1986) 137–46.
11. Daemrich, K.F., Eggert, W.D. & Kohlhase, S., Investigations on irregular waves in hydraulic models. *Proc. 17th Int. Conf. on Coastal Engineering, Sydney, ASCE*, **1** (1980) 186–203.
12. Nielsen, P., Local approximations: A new way of dealing with irregular waves. *Proc. 20th Int. Conf. on Coastal Engineering, Taipei*, **1** (1986) 633–46.
13. Nielsen, P., Analysis of natural waves by local approximations. *J. Waterway, Port, Coastal and Ocean Engineering*, **115** (1989) 384–96.
14. Fenton, J.A., Polynomial approximation and water waves. *Proc. 20th Int. Conf. on Coastal Engineering, Taipei, ASCE*, **1** (1986) 193–207.
15. Sobey, R.J., Variations on Fourier wave theory. *Int. J. Numer. Meth. in Fluids*, **9** (1989) 1453–67.
16. Longuet-Higgins, M.S., Integral properties of periodic gravity waves of finite amplitude. *Proc. Roy. Soc. London, Series A*, **342** (1975) 157–74.
17. Tørum, A. & Skjelbreia, J.E., Irregular water wave kinematics. *Proc. NATO Advance Research Workshop on Water Wave Kinematics, Molde, Norway*, ed. A. Tørum and O. Gudmestad, Kluwer Academic Publishers, Dordrecht, The Netherlands, pp. 281–95.